Specialized Electrophysiological Properties of Anatomically Identified Neurons in the Hilar Region of the Rat Fascia Dentata

JOACHIM LÜBKE,[1] MICHAEL FROTSCHER,[1] AND NELSON SPRUSTON[2,3]
[1]*Anatomisches Institut, Albert-Ludwigs-Universität Freiburg, D-79104 Freiburg;* [2]*Max-Planck-Institut für Medizinische Forschung, Abteilung Zellphysiologie, D-69120 Heidelberg, Germany; and* [3]*Department of Neurobiology and Physiology, Institute for Neuroscience, Northwestern University, Evanston, Illinois 60208-3520*

Lübke, Joachim, Michael Frotscher, and Nelson Spruston. Specialized electrophysiological properties of anatomically identified neurons in the hilar region of the rat fascia dentata. *J. Neurophysiol.* 79: 1518–1534, 1998. Because of their strategic position between the granule cell and pyramidal cell layers, neurons of the hilar region of the hippocampal formation are likely to play an important role in the information processing between the entorhinal cortex and the hippocampus proper. Here we present an electrophysiological characterization of anatomically identified neurons in the fascia dentata as studied using patch-pipette recordings and subsequent biocytin-staining of neurons in slices. The resting potential, input resistance (R_N), membrane time constant (τ_m), ''sag'' in hyperpolarizing responses, maximum firing rate during a 1-s current pulse, spike width, and fast and slow afterhyperpolarizations (AHPs) were determined for several different types of hilar neurons. Basket cells had a dense axonal plexus almost exclusively within the granule cell layer and were distinguishable by their low R_N, short τ_m, lack of sag, and rapid firing rates. Dentate granule cells also lacked sag and were identifiable by their higher R_N, longer τ_m, and lower firing rates than basket cells. Mossy cells had extensive axon collaterals within the hilus and a few long-range collaterals to the inner molecular layer and CA3c and were characterized physiologically by small fast and slow AHPs. Spiny and aspiny hilar interneurons projected primarily either to the inner or outer segment of the molecular layer and had a dense intrahilar axonal plexus, terminating onto somata within the hilus and CA3c. Physiologically, spiny hilar interneurons generally had higher R_N values than mossy cells and a smaller slow AHP than aspiny interneurons. The specialized physiological properties of different classes of hilar neurons are likely to be important determinants of their functional operation within the hippocampal circuitry.

INTRODUCTION

The hilar region of the hippocampus is likely to play an important role in processing information as it travels through the hippocampal formation and therefore may be important for the formation of memories that occurs in the hippocampus (see Buckmaster and Schwartzkroin 1994). Furthermore, neurons in this region were shown to degenerate in temporal lobe epilepsy of humans (de Lanerolle et al. 1989) and experimentally induced epilepsy in rats (Scharfman and Schwartzkroin 1990; Sloviter 1987, 1991). Hilar neurons are also extremely vulnerable to kindling and ischemia (Benviniste and Diemer 1988; Cavazos and Sutula 1990; Crain et al. 1988; Hsu and Buzsáki 1993). Despite the importance of this region, the physiological and morphological properties of the different cell types in the hilus are not as well characterized as those of the principal cell types in the hippocampal formation (Amaral and Witter 1989, 1995; Jonas et al. 1993; Li et al. 1994; Lorente de Nó 1934; Ramón y Cajal 1911; Sik et al. 1993; Spruston and Johnston 1992).

Studies of the dendritic morphology of hilar neurons (Amaral 1978; Frotscher et al. 1991; Lübbers and Frotscher 1987; Ribak and Seress 1983, 1988) and their immunoreactivity for neuronal transmitters and neuropeptides (e.g., Buckmaster et al. 1994; Hendry and Jones 1985; Léránth and Frotscher 1986; Léránth et al. 1984, 1988, 1990; Sloviter and Nilaver 1987; Soriano and Frotscher 1994) have revealed that the population of neurons in the hilus is very heterogeneous, which probably accounts in part for the lack of a detailed characterization of the electrophysiology and axonal projections of these neurons. In addition, the connections of these neurons are difficult to characterize because of the lack of laminated axonal efferents and afferents like those to and from the principal hippocampal cell types. Recently, intracellular labeling studies have shown that the axons of hilar interneurons preferentially terminate in different strata (Buckmaster and Schwartzkroin 1995a,b; Han et al. 1993; Mott et al. 1997; Sik et al. 1997). These studies suggest that there are distinct organizational principles that can be identified by studying the axonal projections of hilar neurons.

To better understand the role of hilar neurons within the hippocampal network, it is important that the physiological properties of the various cell types in the hilus be elucidated. We therefore have correlated the morphology, physiology, and axonal projections of hilar neurons using a combination of patch-pipette recordings and intracellular labeling with biocytin.

METHODS

The methods employed for this study are identical to those described in a related paper on stratum lucidum neurons (Spruston et al. 1997). Abbreviated methods are presented here; for more details, see Spruston et al. (1997).

Patch-pipette recordings and biocytin filling

Transverse hippocampal slices (300–400 μm) were prepared from 13- to 35-day-old Wistar rats. Slices were visualized using infrared differential interference contrast (IR-DIC) videomicroscopy (Stuart et al. 1993). An attempt was made to record only from neurons $\geq$50 μm below the surface of the slice to reduce the probability that dendrites or axon collaterals were severed during slicing. However, neurons deeper than ~100 μm were difficult to

visualize, so most recordings were made from neurons 50–100 μm below the surface of the slice. Patch-pipette recordings were made using electrodes pulled from borosilicate glass and having resistances of 3–10 MΩ when filled with an internal solution containing (in mM) 115 K-gluconate, 20 KCl, 10 Na-phosphocreatine, 0.5 ethylene glycol-bis(β-aminoethyl ether)-*N,N,N′,N′*-tetraacetic acid (EGTA), 10 *N*-2-hydroxyethylpiperazine-*N′*-2-ethanesulfonic acid, 4 Mg^{2+}-ATP, and 0.3 GTP plus 50 units/ml creatine phosphokinase and 5 mg/ml biocytin, adjusted to pH 7.3 with KOH. In most cases, the pipette solution contained 0.5 mM EGTA, but in some recordings 10 mM EGTA was used instead. With the exception of the granule cell shown in Fig. 1, all recordings shown are from cells where 0.5 mM EGTA was present in the pipette. Recordings were made using an Axoclamp 2B amplifier in the bridge voltage-recording mode. Series resistance varied between 5 and 50 MΩ in different recordings. The bath solution contained (in mM) 125 NaCl, 25 $NaHCO_3$, 25 glucose, 2.5 KCl, 1.25 NaH_2PO_4, 2 $CaCl_2$, and 1 $MgCl_2$ and was bubbled with a 95% O_2-5% CO_2 gas mixture. In most experiments, 10 μM 6-cyano-7-nitroquinoxaline-2,3-dione (Tocris), 50 μM D-2-amino-5-phosphonopentanoic acid (Tocris), and 10 μM bicuculline methiodide (Sigma) were included in the extracellular solution to block spontaneous synaptic activity. Recordings were made at physiological temperature (35–37°C).

Data acquisition and analysis

Voltage recordings were filtered at 3–10 kHz and acquired online using a VME-bus computer system. Data analysis was performed using Igor Pro (Wavemetrics) on a Power Macintosh computer using analysis procedures identical to those previously described for neurons in the stratum lucidum region (Spruston et al. 1997). The membrane time constant (τ_m) was estimated from the slowest time constant (τ_0) of exponential fits to the voltage transients in the linear region of the voltage-current plots with the previously described criteria for linearity (Spruston and Johnston 1992; Spruston et al. 1997). The membrane time constant could not be determined in a few cells that did not meet these criteria for linearity. ''Sag'' was quantified by the ratio of the steady state voltage to the peak voltage in response to current injections of −50 to −300 pA. The maximum firing rate was determined as the maximum number of action potentials that could be elicited by a 1-s depolarizing current injection (100–1,000 pA). The slow afterhyperpolarization (AHP) was measured as the most negative membrane potential (relative to the resting potential) after the maximum train of action potentials. Action potential half width and fast AHP were measured from the first action potential with a current injection just above threshold. Action potential amplitude and fast AHP were measured relative to the action potential threshold. All statistical analyses were performed using single factor analysis of variance with Tukey's multiple comparisons. Differences were regarded as statistically significant at the $P < 0.05$ level.

Morphological analysis

During recording, cells were filled with 0.5% biocytin (15–30 min) to reveal their morphology. At the end of the recording, slices were immersion-fixed in a phosphate buffered solution containing 2% paraformaldehyde and 1% glutaraldehyde (100 mM; pH 7.4) overnight. Slices then were processed using an avidin-horseradish peroxidase (HRP), avidin-biotin-complex (ABC)-solution (1:150, Vector Laboratories) as described (Lübke et al. 1996). Representative examples of well-filled hilar neurons and granule cells were examined with an Olympus BX 50 microscope, photographed, and drawn with a camera lucida at a final magnification of ×480.

RESULTS

Morphological identification of hilar neurons

Some morphological features of hilar neurons could be distinguished in the living slice using IR-DIC videomicroscopy. Putative basket cells were identified by their relatively large somata and position adjacent to the granule cell layer. Putative mossy cells could be identified by their large ovoid or triangular somata, although in some cases, further morphological analysis after biocytin staining revealed that these cells lacked the dense thorny spines characteristic of mossy cells. We could not distinguish between other spiny and aspiny hilar neurons using IR-DIC videomicroscopy alone. Recordings therefore were made from neurons in all areas of the hilus. Successful morphological identification of cell type was achieved in >90% of biocytin-filled neurons after avidin-HRP staining and light microscopic examination of somatic shape and location, dendritic arborization, and axonal projection. The morphological and physiological properties are described here for six types of neurons: dentate granule cells, dentate basket cells, hilar mossy cells, spiny hilar interneurons, and aspiny hilar interneurons projecting either to the inner molecular layer (IML) or outer molecular layer (OML).

Dendritic arborizations and axonal projection of dentate granule cells

Although not part of the hilar region, granule cells of the fascia dentata were characterized because they are an integral part of the circuitry of the hilus (Frotscher et al. 1994; Lindsay and Scheibel 1981; Lorente de Nó 1934; Lübbers and Frotscher 1987; Seress and Pokorny 1981). Also, the inclusion of granule cells in this study facilitated a direct comparison of their physiology to that of the hilar neurons. Morphological analysis revealed that granule cells had their characteristic morphological features that have been well described before (Claiborne et al. 1986, 1990), namely ovoid somata with one or two primary apical dendrites, which branch and fan out to a cone-shaped dendritic field within the molecular layer (Fig. 1*A*). The main granule cell axon entered the hilus and gave rise to several mossy fiber collaterals (Fig. 1*A*). The main axon could be followed long distances running parallel to CA3c the pyramidal layer while giving off several short terminal branches. Both the main axon and axon collaterals gave rise to mossy fiber boutons spaced ~20 μm apart.

Notably, one cell was rejected from the granule cell data set because its soma was very small, and its dendrites were thin and aspinous, and R_N was considerably larger than that of other neurons in the granule cell layer (R_N = 1.2 GΩ; τ_o = 50 ms). The morphology of this neuron is reminiscent of the VIP-immunoreactive or the choline acetyltransferase-immunoreactive neurons found in the granule cell layer (Frotscher et al. 1986; Sloviter and Nilaver 1987).

Physiology of dentate granule cells

An example of the physiological properties of a dentate granule cell is shown in Fig. 1, *B–D*. At the maximum firing rate, little spike frequency accommodation is apparent

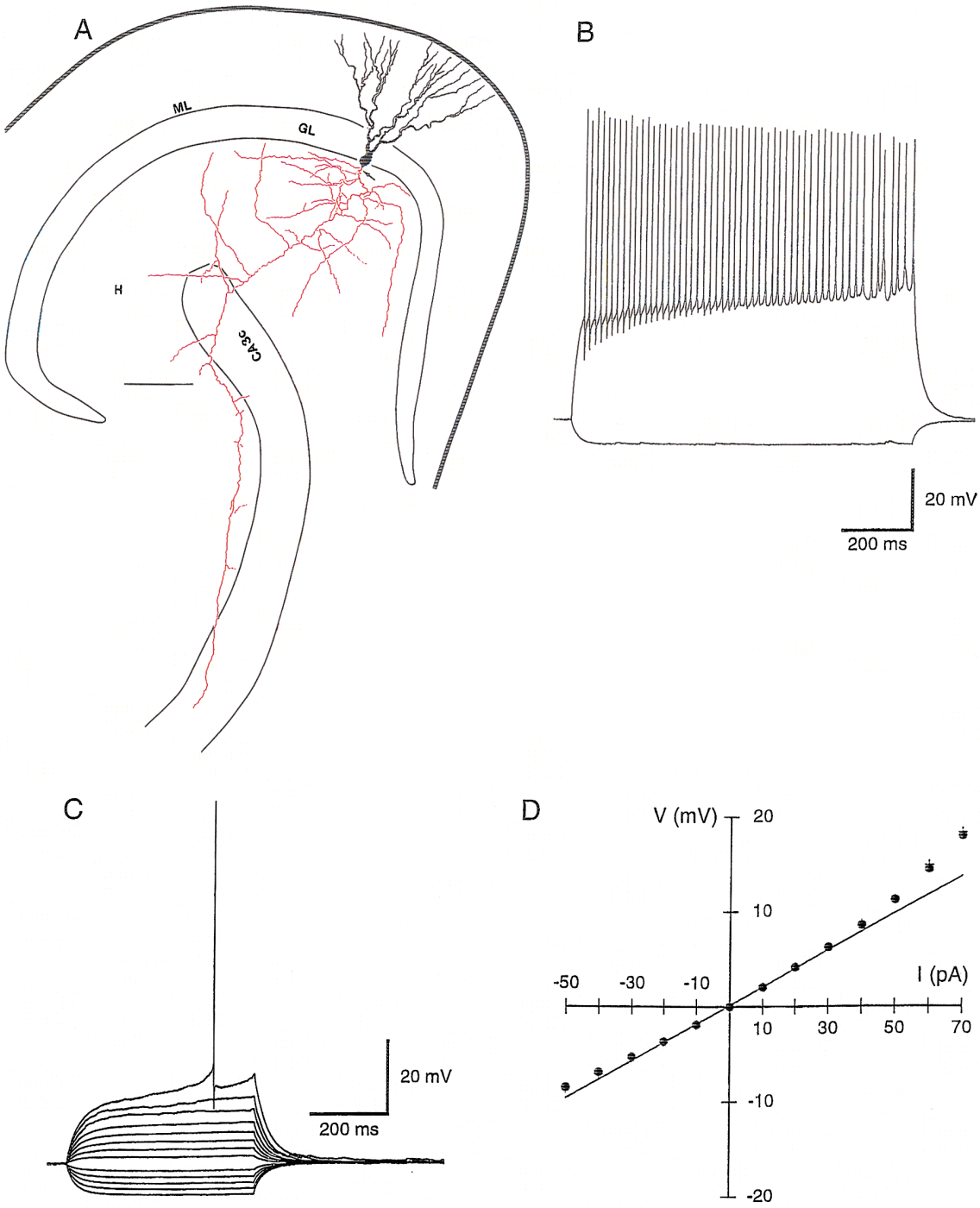

FIG. 1. Paired morphology and physiology of a dentate granule cell. *A*: morphology of the biocytin-filled neuron. Dendrites (black) form a characteristic cone-shaped dendritic tree. Several axon collaterals (red) project deep into the hilus with the main axon projecting toward the pyramidal cell layer. →, origin of the axon from the cell body; thick black line indicates the pial surface. H, hilar region; GL, granule cell layer; ML, molecular layer. Scale bar: 100 μm. *B*: responses to 1-s current injections of +250 and −50 pA. Maximum firing (54 Hz) was observed with the +250-pA current injection. Sag ratio = 1.0 (−50 pA response). *C*: voltage responses to current injections of −50 to +80 pA in 10-pA increments. Responses from −50 to +50 pA are averages of 11–22 trials; responses from +60 to +80 pA are single trials. τ_o = 31 ms; action potential half-width = 0.67 ms. *D*: voltage-current relationship for the data shown in *C*. ●, steady state voltages; +, peak responses, most of which overlap; ——, linear regression through the steady state points between −20 and +20 pA. R_N = 195 MΩ; V_{rest} = −77 mV.

because the patch pipette contained 10 mM EGTA. In other neurons recorded with 0.5 mM internal EGTA, more accommodation was observed, but the maximum number of spikes during a 1-s current injection was not significantly different. Also of note is that granule cells displayed little or no sag during hyperpolarizing voltage changes (Fig. 1, *B* and *C*).

TABLE 1. *Physiological properties of neurons in the hilus and fascia dentata of the hippocampal formation*

Cell Type	*n**	Resting Potential, mV	R_N, MΩ	τ_0, ms	Sag Ratio	Maximum Firing Rate, s^{-1}	Spike Width, ms	Fast AHP, mV	Slow AHP, mV
Granule cells	16 (16)	−75 ± 2	292 ± 34	31 ± 2	0.97 ± 0.01	72 ± 8	0.87 ± 0.06	−11.7 ± 1.1	−0.6 ± 0.4
		−86, −60	111, 650	16, 43	0.93, 1.02	39, 128	0.53, 1.48	−22.5, −3.4	−2.6, 1.2
Basket cells	3 (3)	−62 ± 3	43 ± 5	10 ± 1	0.97 ± 0.02	230 ± 15	0.25 ± 0.04	−20 ± 2.3	−2.3 ± 0.2
		−66, −56	32, 54	9, 11	0.91, 1.00	212, 266	0.18, 0.33	−24.9, −14.9	−2.8, −1.9
Mossy cells	9 (8)	−62 ± 1	199 ± 19	41 ± 3	0.81 ± 0.03	50 ± 6	0.78 ± 0.04	−6.2 ± 0.9	−2.8 ± 0.7
		−67, −55	83, 287	24, 52	0.66, 0.91	33, 83	0.53, 0.96	−11.8, −2.9	−6.0, 0.7
Spiny interneurons	3 (2)	−65 ± 6	371 ± 47	35 ± 0	0.82 ± 0.02	69 ± 4	0.72 ± 0.08	−13.1 ± 3.0	−3.1 ± 1.0
		−75, −50	286, 480	35, 35	0.78, 0.86	61, 77	0.53, 0.87	−20.0, −7.2	−5.2, −1.1
IML aspiny interneurons	4 (4)	−64 ± 2	363 ± 62	30 ± 6	0.80 ± 0.04	81 ± 9	0.50 ± 0.02	−12.3 ± 2.3	−9. ± 2.7
		−68, −59	194, 516	11, 41	0.68, 0.89	58, 108	0.44, 0.55	−18.7, −6.0	−14.7, −1.3
OML aspiny interneurons	2 (1)	−68 ± 2	284 ± 89	15	0.84 ± 0.06	101 ± 24	0.62 ± 0.18	−16.8 ± 1.8	−7.5 ± 4.6
		−70, −65	158, 410	15	0.76, 0.92	66, 135	0.37, 0.87	−19.4, −14.2	−14.0, −0.9

For each parameter, mean ± SD and range (low, high) are indicated. IML and OML, inner and outer molecular layer. * The *n* value for τ_0 is indicated in parentheses; see METHODS for explanation.

The physiological properties of 16 granule cells are summarized in Table 1. The values for τ_o and R_N are in reasonable agreement with those determined previously (Spruston and Johnston 1992; Staley et al. 1992). Granule cells typically had resting potentials that were more negative than the other cell types studied. This difference was statistically significant for all cell types except spiny hilar interneurons. Considerable overlap in the ranges of resting potentials, however, makes it impossible to identify a granule cell with certainty on the basis of resting potential. Granule cells could be distinguished, however, on the basis of a combination of resting potential, lack of sag in hyperpolarizing responses, and maximum firing rate, which was substantially lower than the only other cell type lacking sag, namely basket cells (see further).

Basket cells with axonal projection to the granule cell layer

A representative example of a basket cell is given in Figs. 2*A* and 3*A*. Interneurons of this type resemble those described in the early Golgi studies by Ramón y Cajal (1911) and Lorente de Nó (1934) and in later Golgi, Golgi/electron microscopic, and immunocytochemical studies (Amaral 1978; Lübbers and Frotscher 1987; Ribak and Seress 1983; Ribak et al. 1978; Seress and Frotscher 1991; Seress and Pokorny 1981). All basket cells ($n = 6$) were located 10–20 μm from the granule cell layer on the hilar side. Basket cells had large, round, ovoid or triangular somata, 20–25 μm in diameter. A thick main apical dendrite ascends through the granule cell layer where it branches off into thick secondary dendrites, which then terminate in the molecular layer, often with a terminal tuft (Fig. 2*A*). Two to six basal dendrites emerge from the base of the soma and extend toward the hilar region. The dendrites of all cells were aspiny, but spine-like or hair-like protrusions were found on secondary dendrites and the terminal tufts. Dendritic varicosities were found mainly on basal dendrites (Fig. 2*A*).

The main axon emerges directly from one side of the cell body (Figs. 2*A* and 3*A*) or from one of the primary dendrites. It then follows the course of the main apical dendrites into the granule cell layer where it gives rise to several thick secondary collaterals, which then branch off into further tangentially or vertically oriented collaterals, which invade nearly the entire area of the granule cell layer (Figs. 2*A* and 3*A*). The axonal projection of all basket neurons investigated was restricted to the granule cell layer with one exception. The neuron shown in Figs. 2*A* and 3*A* sends off two secondary axonal collaterals through the granule cell layer, which then branch off and terminate within the innermost portion of the molecular layer. The axons of basket cells were seen clearly to form basket-like bouton arrays (3–6 contacts/neuron) on granule cell somata (Fig. 2*B*). In contrast to the other hilar interneurons, no axonal collaterals were seen within the hilar region.

Physiology of basket cells

An example of a recording from a basket cell is shown in Fig. 3, *B–D*, and a summary of the physiological properties determined from three such recordings is given in Table 1. Basket cells displayed several characteristic physiological properties. The maximum number of action potentials during a 1-s current injection was significantly higher and the action potential half-width significantly narrower than any of the other cell types studied. In addition, R_N was lower and τ_o faster than for the other cell types in the hilar region. Most of these differences were statistically significant except for the difference in R_N between basket cells and mossy cells. The combination of these differences are distinctive enough that any single basket cell recording is clearly distinguishable from other hilar neurons on the basis of the physiology alone.

Mossy cells with local axonal collaterals in the hilus

Besides granule cells, the major spiny cell type of the fascia dentata are the mossy cells (Amaral 1978; Buckmaster et al. 1993a,b, 1996; Frotscher et al. 1991; Ribak et al. 1985; Scharfman 1995; Soriano and Frotscher 1994). Mossy cells were identified by the dense ''thorny excrescences'' covering their dendrites (Figs. 4*A*, *inset*, and 5*A*). Mossy cells were encountered throughout the entire hilar region, although they were more prominent near the granule cell layer. They are large, multipolar or fusiform neurons; from the

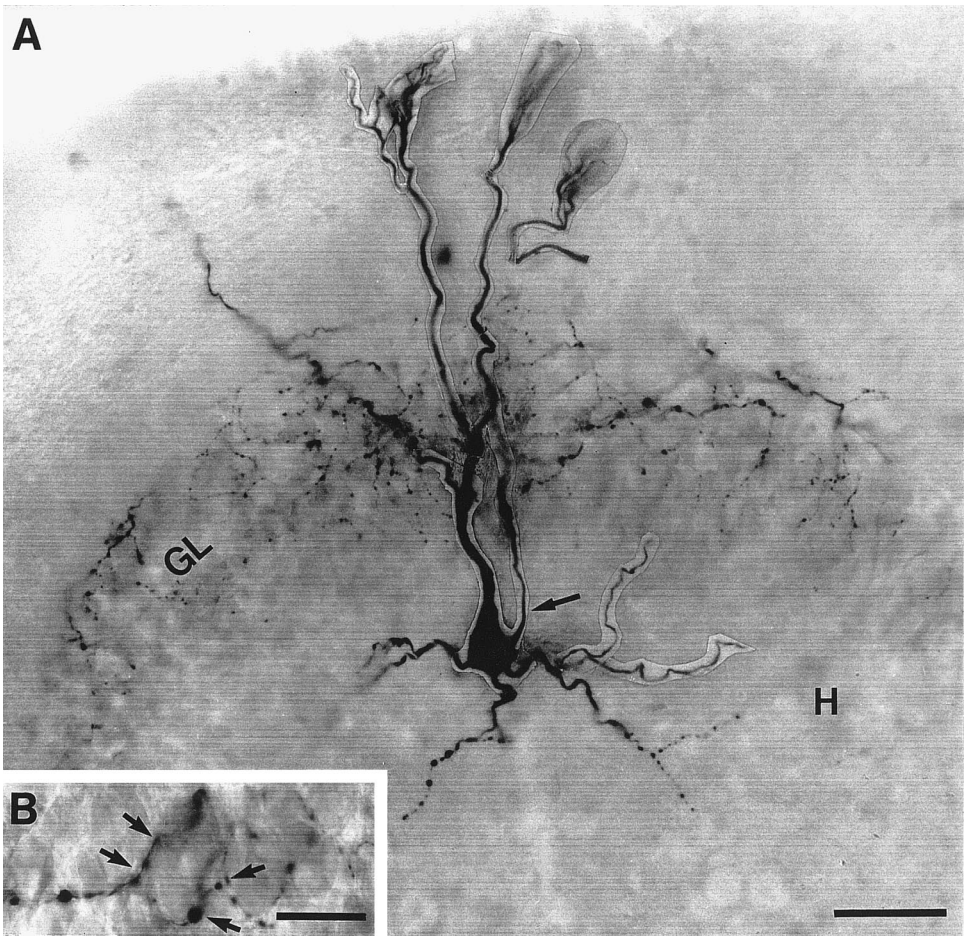

FIG. 2. Representative example of a dentate basket cell. *A*: photomontage of the basket cell the camera lucida reconstruction and physiology of which is shown in Fig. 3. Note extensive axonal arborization in the granule cell layer of fascia dentata. *B*: high magnification of pericellular ''basket'' of boutons formed by a single collateral on the cell body of a granule cell. GL, granule cell layer; H, hilar region. Scale bar in *A*: 100 μm; *B*: 50 μm.

ovoid cell body up to seven thick primary dendrites originate, which usually bifurcate and give rise to several secondary and tertiary branches (Fig. 4, *A* and *B*, and 5*A*). Depending on the location of the neurons within the hilus, mossy cell dendrites run in different directions. Dendrites of neurons situated beneath the granule cell layer tend to run parallel to the granule cell layer (Figs. 4*A* and 5*A*). Mossy cells located more deeply in the hilus extend dendrites in all directions (Fig. 4*B*). Some dendritic branches pass through the granule cell layer, terminating in the inner molecular layer (not shown).

The main axon originates from either the cell body or one of the primary dendrites (Figs. 4*A* and 5*A*). It can be followed over a long distance within the hilus but finally leaves the hippocampus via the alveus. Shortly after its origin, the main axon gives rise to several very long axonal collaterals, most of which remain within the hilus, often spanning the entire hilar area (Figs. 4*C* and 5*A*). Some of the collaterals follow a course more or less parallel to the granule cell layer with lengths $\leq$900 μm (Fig. 5*A*). Other axon collaterals could be followed entering and terminating within the CA3c pyramidal cell layer (Fig. 4*E* and 5*A*) or passing through the granule cell layer (Fig. 4*D*) and then taking a course parallel to the granule cell layer within the inner molecular layer (Fig. 4, *F* and *G*). The projection toward the inner molecular layer and CA3c seems to be variable between mossy cells, at least as far as it could be followed in the slice.

Physiology of mossy cells

An example of the physiological properties of a mossy cell is shown in Fig. 5, *B–D*, and the summary of the properties measured from nine neurons is given in Table 1. Mossy cells had the lowest firing rate, on average, but this difference was only statistically significant for the comparison with basket cells. Action potentials in mossy cells also had the smallest fast AHPs. Our data indicate, however, that some of these differences are not statistically significant and that there is considerable overlap in the ranges of these parameters measured from mossy cells and other hilar neurons. The difference in mossy cell firing rate and spike width was only statistically significant for the comparison with basket cells, and the difference in fast AHP was significant for the comparison with basket cells and granule cells but not with spiny and IML aspiny hilar interneurons. Mossy cells had the slowest τ_o values of the neurons characterized, yet had lower R_N than all other cell types except basket cells, presumably because of the large somata and extensive dendritic arborizations in these cells. The sag in hyperpolarizing responses was prominent in mossy cells, which distinguished them from basket cells

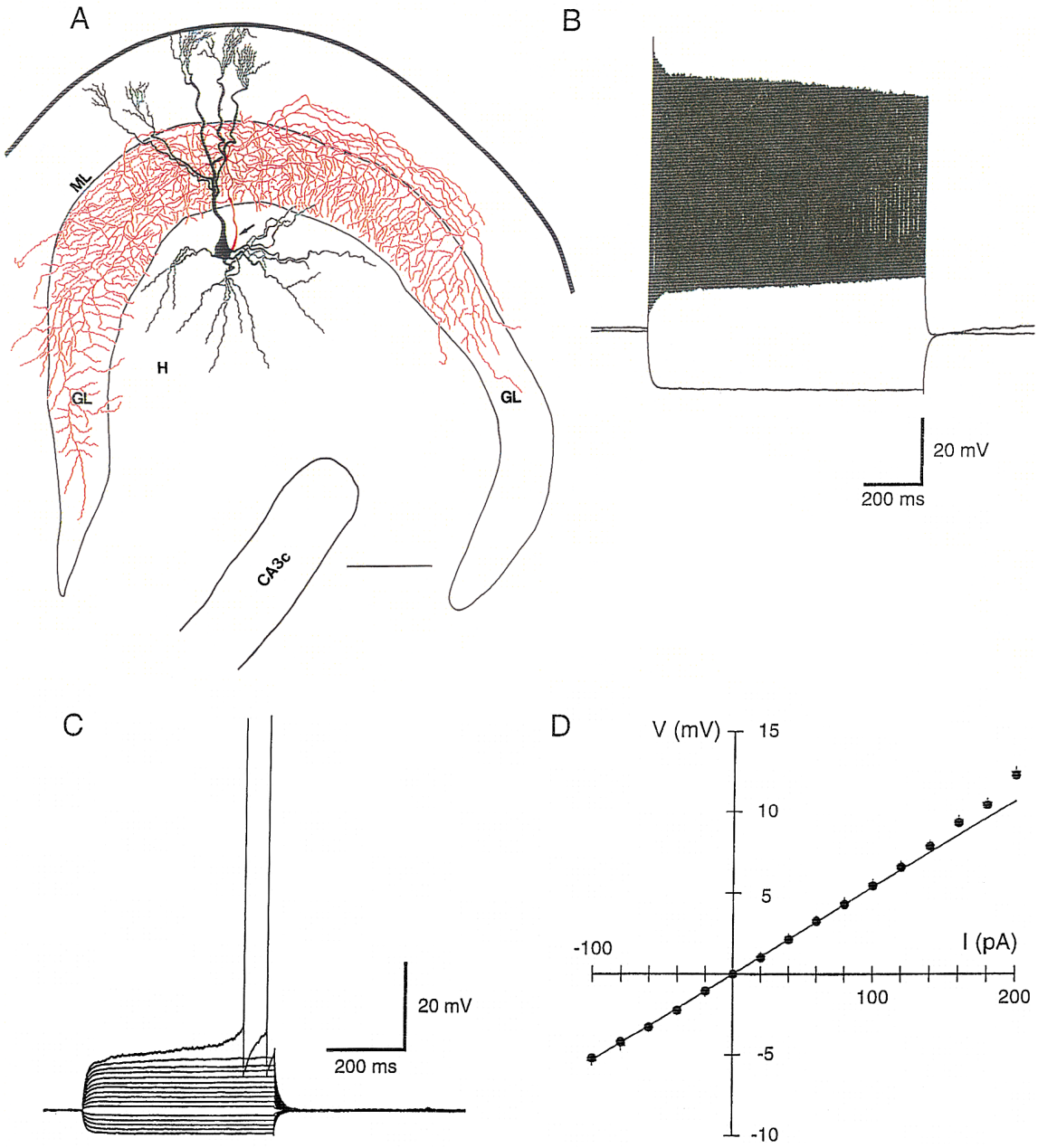

FIG. 3. Paired morphology and physiology of a dentate basket cell. *A*: camera lucida reconstruction of the biocytin-filled basket cell shown in Fig. 2. Axonal projection (red) of the neuron is restricted mainly to the granule cell layer, although a few axonal collaterals enter the innermost portion of the molecular layer. Axonal collaterals extend along approximately two-thirds of the length of the granule cell layer. →, origin of the axon from the cell body; thick black line indicates the pial surface. H, hilar region; GL, granule cell layer; ML, molecular layer. Scale bar: 100 μm. *B*: responses to 1-s current injections of +900 and −300 pA. Maximum firing (266 Hz) was observed with the +900-pA current injection. Sag ratio = 0.99 (−300 pA response). *C*: voltage responses to current injections of −100 to +220 pA in 20-pA increments. All responses, except the action potentials, are averages of 4–15 trials. τ_o = 11 ms; action potential half-width = 0.33 ms. *D*: voltage-current relationship for the data shown in *C*. ●, steady state voltages; +, peak responses, most of which overlap; ——, linear regression through the steady state points between −100 and +120 pA. R_N = 54 MΩ; V_{rest} = −52 mV.

and granule cells (which lack sag) but not from spiny or aspiny hilar interneurons. In fact, the combination of physiological properties made it generally easy to distinguish mossy cells from granule cells or basket cells but overlapped enough with spiny and aspiny interneurons that it is difficult to identify mossy cells on the basis of spike firing and passive membrane properties alone.

Spiny hilar interneurons with axonal projections to the outer molecular layer

In our sample, we identified three spiny interneurons that were distinguishable from mossy cells. These neurons lacked the characteristic excrescences of mossy cells, had somewhat smaller somata, longer and thinner spines than mossy cells,

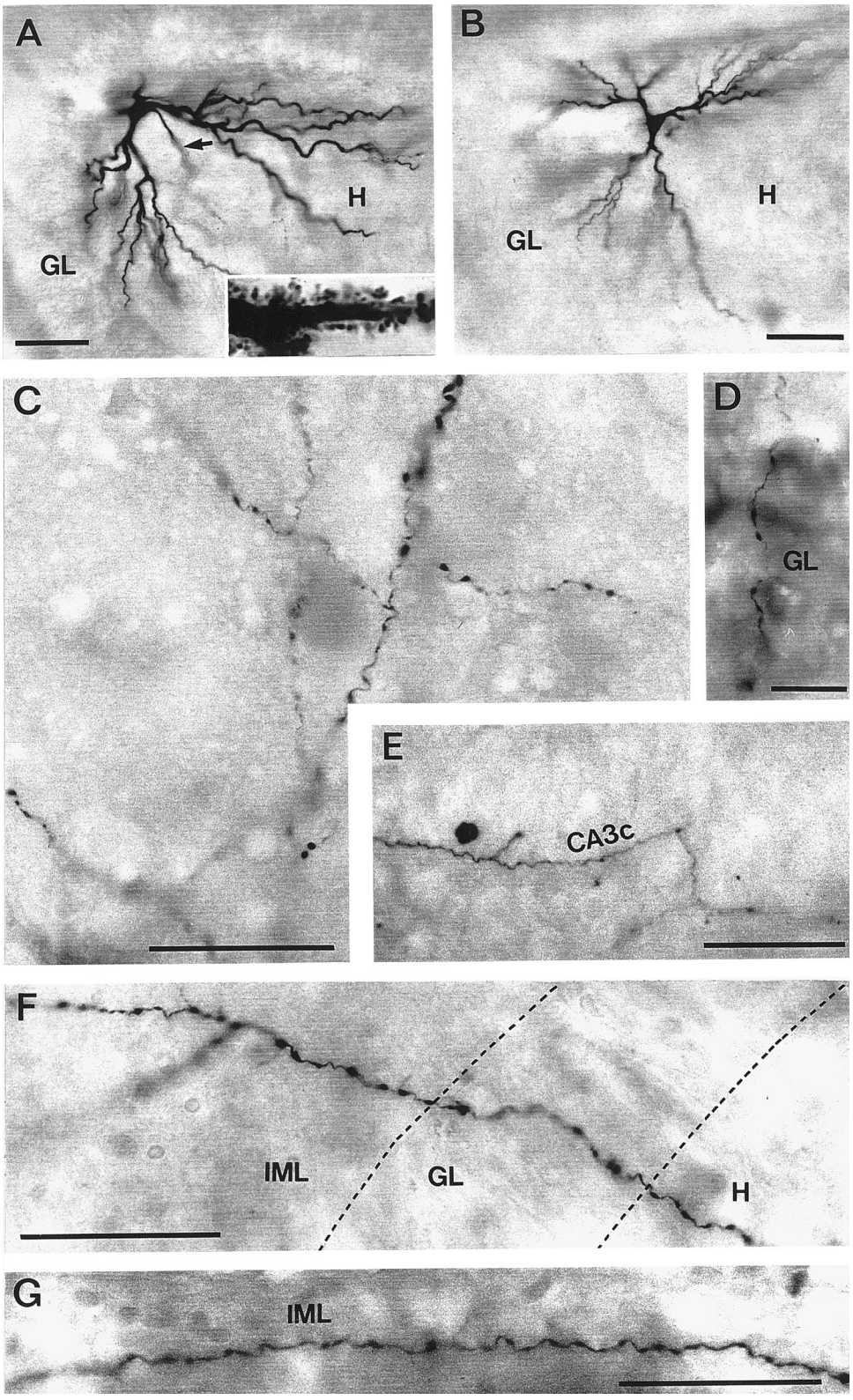

FIG. 4. Morphological characteristics of hilar mossy cells. *A* and *B*: 2 examples of hilar mossy cells at low magnification to show the different arrangement of the dendritic tree. →, main axon. *Inset*: high magnification of the typical excrescences on proximal mossy cell dendrites. *C*: local hilar collaterals of a mossy cell. *D*: single collateral of a mossy cell with en passant boutons traversing the granule cell layer toward the inner molecular layer. *E*: single axon collateral of a mossy cell entering and terminating within the pyramidal layer of CA3c. *F* and *G*: 2 examples of single, mossy cell collaterals leaving the hilus, ascending through the granule cell layer, and finally terminating in the inner molecular layer. H, hilar region; GL, granule cell layer; IML, inner molecular layer. Scale bars in *A* and *B*: 100 μm; *C*–*G*: 50 μm.

and had an axonal projection pattern that differed markedly from that of the mossy cells. An example of such a spiny interneuron is shown in Fig. 6*A*. The soma of this neuron is situated near the granule cell layer. Several primary dendrites emerge from the poles of the fusiform cell body, some of which bifurcate into two long secondary branches running within the hilar region or passing through the granule cell layer toward the molecular layer (Fig. 6*A*). The distal portions of all dendrites are covered with numerous long, thin spines.

The main axon emerges directly from one pole of the

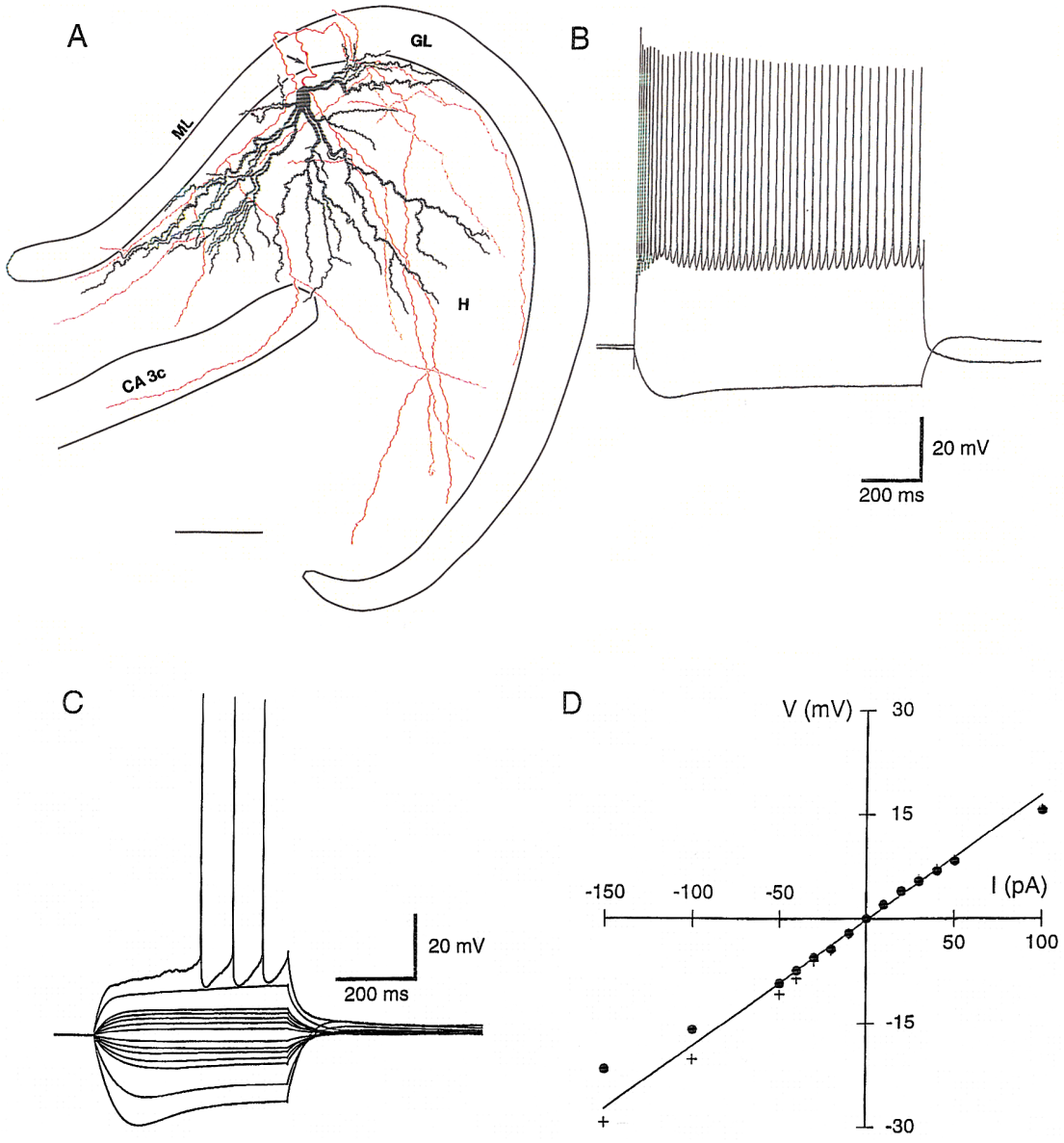

FIG. 5. Paired morphology and physiology of a hilar mossy cell. *A*: morphology of the biocytin-filled neuron. Axonal projection of the neuron (red) is restricted mainly to the hilus with some collaterals projecting to CA3c. →, origin of the axon from the cell body. H, hilar region; GL, granule cell layer; ML, molecular layer. Scale bar: 100 μm. *B*: responses to 1-s current injections of +1,000 and −300 pA. Maximum firing (44 Hz) was observed with the +1,000-pA current injection. Sag ratio = 0.75 (−300 pA response). *C*: voltage responses to current injections of −150 to +150 pA in 50-pA increments and −40 to +40 pA in 10-pA increments. All responses, except the action potentials, are averages of 5–15 trials. τ_o = 49 ms; action potential half-width = 0.89 ms. *D*: voltage-current relationship for the data shown in *C*. ●, steady state voltages; +, peak responses, most of which overlap; ——, linear regression through the steady state points between −50 and +50 pA. R_N = 181 MΩ; V_{rest} = −64 mV.

soma and gives rise to several collaterals that pass through the hilus and enter the molecular layer. Most of these collaterals terminate in the outer molecular layer, similar to the axonal projection pattern described for one class of aspiny hilar interneurons (see further, compare Fig. 6*A* with Fig. 8*B*). In addition, a second prominent axonal domain was found in the hilar region with some axonal collaterals terminating in layer CA3c (Fig. 6*A*). These spiny interneurons occasionally form basket-like bouton arrays on granule cell somata and other neurons within the hilar region.

Physiology of spiny hilar interneurons

An example of the physiological properties of a spiny hilar interneuron is shown in Fig. 6, *B–D*, and the properties of three such cells summarized in Table 1. As shown in Fig. 6, these cells reached maximum firing rates of ~70 action potentials during a 1-s current injection, considerably lower than the maximum rate of basket cell action potentials but comparable with the other cell types studied. τ_o and R_N were most similar to that of aspiny hilar interneurons and statistically different only from basket cells. Aside from be-

ing distinguishable from basket cells, spiny hilar interneurons could be distinguished physiologically only from granule cells, on the basis of the presence of a considerable sag in hyperpolarizing responses.

Aspiny interneurons with axonal projection to the inner molecular layer

Hilar interneurons lacking spines fell into two distinct categories: those with axons projecting to the inner molecular layer and those with axons projecting to the outer molecular layer. Examples of each of these two cell types are shown in Figs. 7, 8, *A* and *B*, and 9*A*.

Aspiny interneurons projecting to the inner molecular layer ($n = 4$) were found at different locations within the hilus but usually were situated 10–20 μm beneath the granule cell layer (Fig. 7*A*). These neurons are very variable in their dendritic morphology. They are fusiform or multipolar, with smooth dendrites mainly distributed in the hilus, although some dendrites could be followed to terminate in the molecular layer or in CA3c (Fig. 9*A*).

The main axon of these neurons emerges from the soma or one of the primary dendrites and sends off collaterals that pass through the granule cell layer toward the inner molecular layer where they spread out in a tangentially oriented fashion (Figs. 7*A*, 8*A*, and 9*A*). Several axonal collaterals have vertically oriented side branches, some of which enter and terminate within the middle portion of the molecular layer. The tangential spread of the axonal arbor could reach distances $\leq$1 mm. While passing through the granule cell layer, they establish basket-like boutons around granule cell somata (Fig. 7*A*, *inset*). A second population of axonal collaterals found within the hilus (Figs. 7*B*, 8*A*, and 9*A*) is variable in density and range. Some of them run parallel to the granule cell layer for a long distance ($\leq$800 μm), whereas others could be followed toward CA3c. Within the hilus, these neurons also form basket-like bouton arrays around somata (Fig. 7*B*, *inset*).

Aspiny interneurons with axonal projections to the outer molecular layer

A representative example of an aspiny hilar interneuron with an axonal projection to the outer molecular layer is given in Fig. 8*B*. These neurons ($n = 4$) usually had somata located within the deep hilus, 20–50 μm beneath the granule cell layer, and were fusiform in shape, with two- to four-thick smooth primary dendrites emerging from the two poles of the soma. After a short distance, these primary dendrites give rise to several secondary and tertiary branches, which either remain within the hilus or terminate in the granule cell layer or molecular layer, sometimes ending in a small terminal tuft (Fig. 8*B*). The characteristic feature of these neurons is their axonal projection terminating in the outer molecular layer in a particular vertically oriented fashion (Fig. 8*B*). The main axon emerges from either the soma or one of the primary dendrites (Fig. 8*B*). Shortly after leaving the soma, the axon gives off several very long axonal collaterals ($\leq$900 μm). One population then takes a more or less vertical course passing through the granule cell layer, the inner molecular layer, and finally terminating within the outer molecular layer. Within the inner molecular layer, some of these collaterals give rise to tangentially oriented side branches of variable length (30–300 μm) that also terminate within the outer molecular layer. On their way through the granule cell layer, these vertically oriented axonal collaterals form basket-like bouton arrays around granule cell somata. A second population of collaterals establishes a sometimes dense axonal plexus within the hilus, with en passant boutons contacting somata of other hilar neurons. Some of these collaterals were seen to project to CA3c (Fig. 8B).

Physiology of aspiny hilar interneurons

The physiological properties obtained from four IML-projecting aspiny interneurons and two OML-projecting aspiny interneurons were similar (Table 1). An example of a recording from an identified IML aspiny neuron is shown in Fig. 9, *B–D*. This neuron is typical of both IML and OML aspiny interneurons in that it fires at moderate rates but exhibits considerable spike frequency accommodation and never approaches the rapid firing rates observed in basket cells. Aspiny hilar interneurons also displayed considerable sag in hyperpolarizing responses and hence could be distinguished from both granule cells and basket cells on the basis of this feature. The most characteristic physiological feature of aspiny interneurons was the large slow AHP after a train of action potentials (Fig. 9, *B–D*, Table 1). One IML and one OML aspiny interneuron, however, had relatively small slow AHP potentials, so it is clear that this parameter is not a perfect fingerprint for these neurons. R_N of IML aspiny interneurons was significantly higher than for basket cells or mossy cells, but there was overlap in the range of values for all cell types except basket cells. τ_o of IML aspiny interneurons was only statistically different from basket cells, and it appeared to be comparable with that of granule cells, mossy cells, and spiny interneurons (Table 1).

DISCUSSION

The role of the hippocampus in information processing is determined by the physiological properties and synaptic connections of its various neuronal types. Our study of identified cell types in the hilar region focused on the axonal plexus and physiological characteristics of the neurons because previous Golgi studies did not provide sufficient staining of the axon of the cells and many physiological studies lacked the identification of cell types. Although our approach has the advantage of visually identifying neurons with infrared-DIC, some caveats should be raised.

First, our approach suffers from the problem that longitudinal connections, which constitute a substantial component of the hippocampal circuitry (Amaral and Witter 1989), could not be examined. Second, speculations about which connections are excitatory or inhibitory remain tentative in the absence of physiological analysis of these connections with paired recordings from morphologically identified neurons. In addition, some hilar neurons are likely to perform neuromodulatory functions, as indicated by the presence of various neuroactive peptides in these cells. Third, our cells are from relatively young animals (2- to 5-wk old), and we

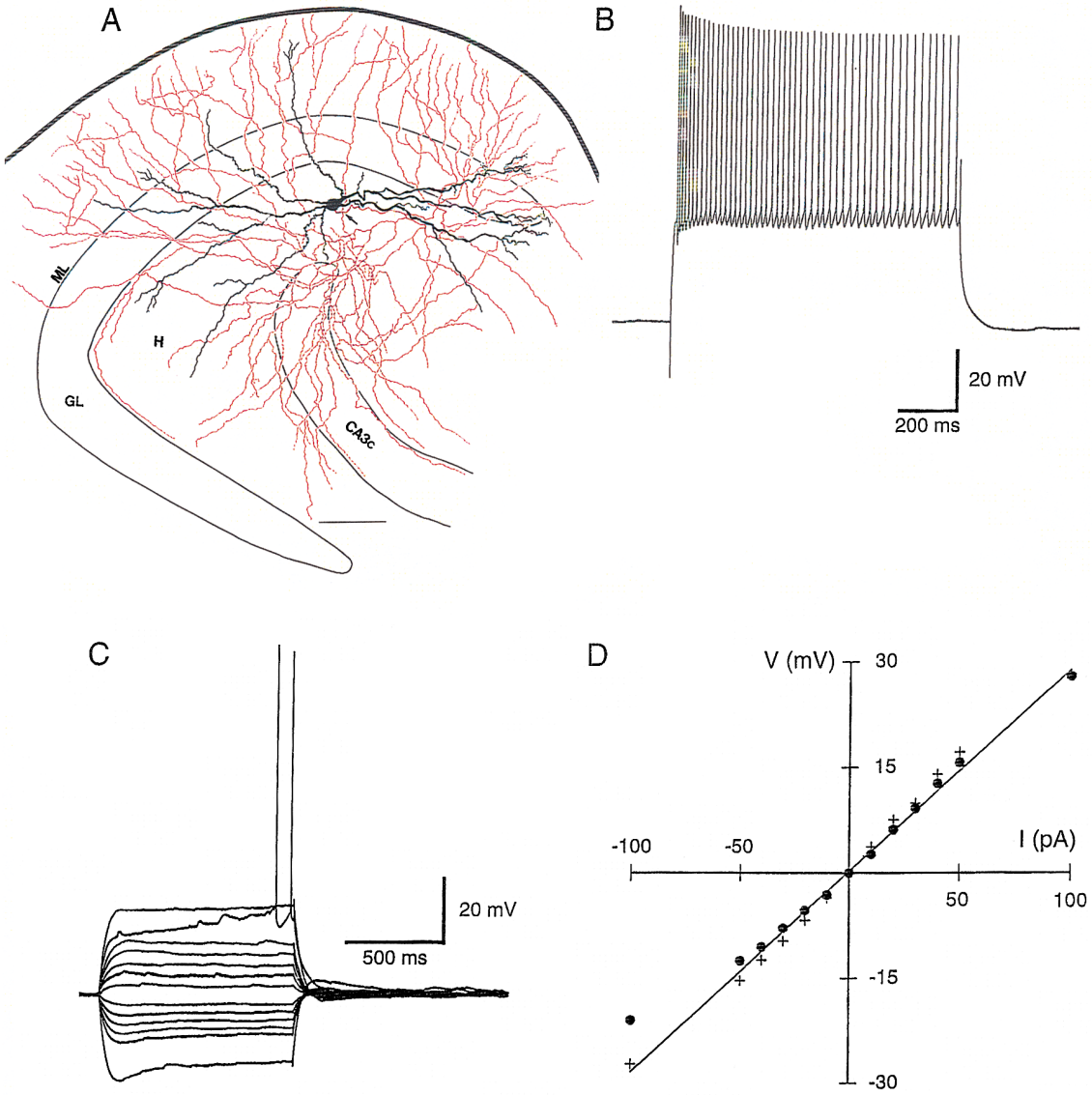

FIG. 6. Paired morphology and physiology of a spiny hilar interneuron. *A*: morphology of the biocytin-filled neuron. Axonal projection (red) to the molecular layer is restricted mainly to the outer zone. Note abundant collaterals in the hilus and in area CA3c. →, origin of the axon from the cell body; thick black line indicates the pial surface. H, hilar region; GL, granule cell layer; ML, molecular layer. Scale bar: 100 μm. *B*: responses to a 1-s current injection of +800 pA. Maximum firing (70 Hz) was observed with the +800-pA current injection. *C*: voltage responses to current injections of −100 to +150 pA in 50-pA increments and −40 to +40 pA in 10-pA increments. All responses, except the 1 containing action potentials, are averages of 4–8 trials. Note that the spikes arise from a slow ramp in response to the +150-pA current injection. Presence of a larger initial depolarization in response to +100 pA suggests that a K^+ current is activated by the larger current injection, which then slowly inactivates, causing the depolarizing ramp response to the +150-pA current injection. τ_o = 35 ms; action potential half-width = 0.87 ms; sag ratio = 0.81 (−100 pA response). *D*: voltage-current relationship for the data shown in *C*. ●, steady state voltages; +, peak responses, most of which overlap; ——, linear regression through the steady state points between −20 and +20 pA. R_N = 286 MΩ; V_{rest} = −71 mV.

cannot exclude that they undergo further physiological and morphological maturation. Fourth, the need to fill the neurons with biocytin precluded the use of perforated-patch recording and hence introduces possible errors in physiological properties as a result of the influence of the pipette solution on the intracellular composition. One such possible problem is the influence of the EGTA in the pipette solution on spike firing properties. Because buffering internal calcium was shown to reduce spike frequency accommodation and AHP (Madison and Nicoll 1984), we used a low concentration of internal EGTA (0.5 mM). To examine the possible effects of internal EGTA, we also compared spike train responses in granule cells with electrodes containing 0.5 and 10 mM EGTA (see also Staley et al. 1992). Although some loss of accommodation was observed with the higher EGTA concentration when using weaker stimulation, no differences between the 0.5 and 10 mM internal EGTA groups were observed when measuring maximum firing rate, fast AHP, or slow AHP using strong depolarizing current pulses. Assuming that the normal calcium-buffering capacity of gran-

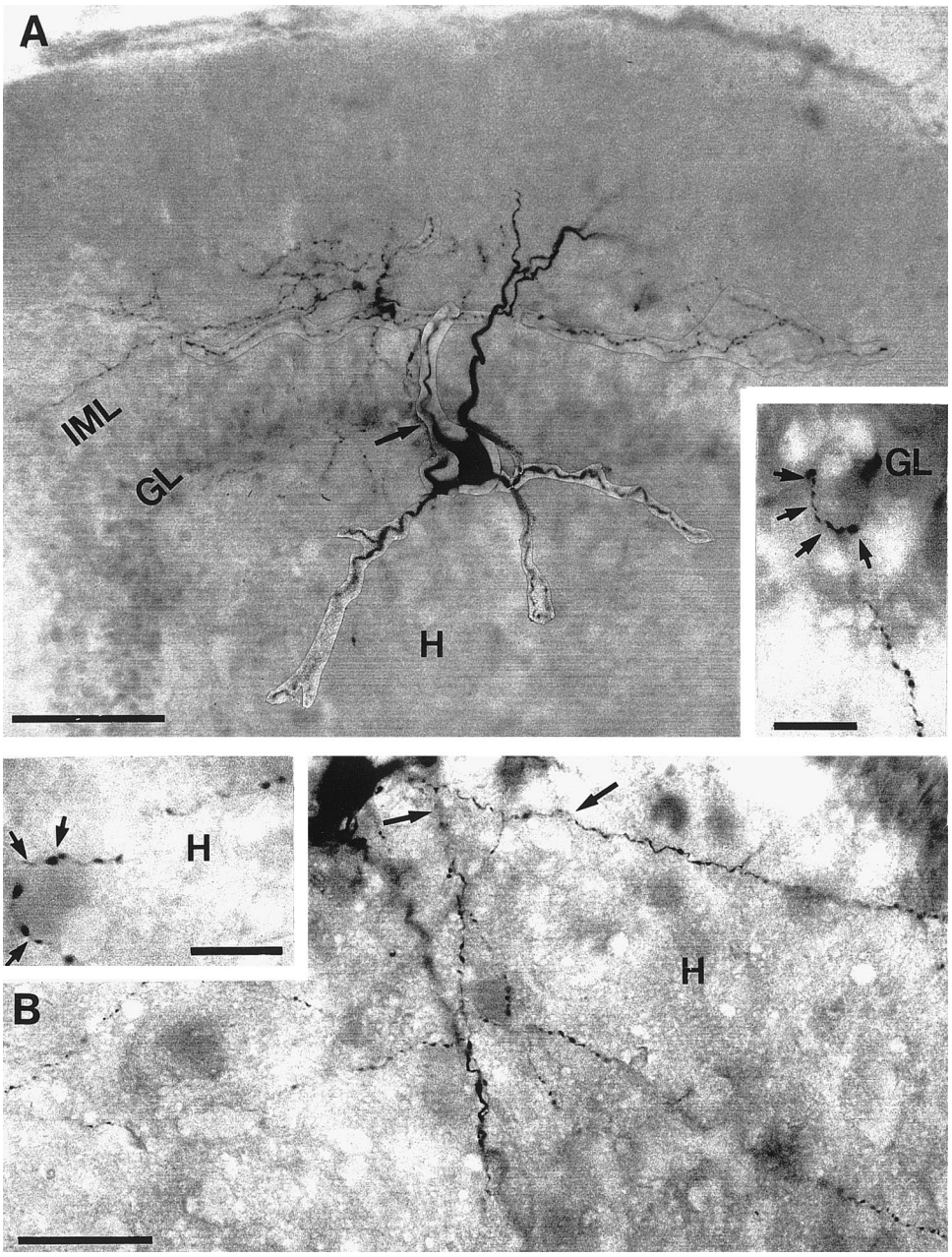

FIG. 7. Representative example of an aspiny hilar interneuron projecting to the inner molecular layer. *A*: photomontage of the neuron at low power. *Inset*: single collateral, which forms a basket-like array of boutons (→) around a granule cell soma. *B*: Hilar collaterals (→) of another neuron projecting mainly to the inner molecular layer. *Inset*: high magnification of a basket-like array of synaptic boutons (→) around the cell body of a hilar neuron. GL, granule cell layer; H, hilar region; IML, inner molecular layer. Scale bars, *A*: 100 μm, *inset* in *A*: 25 μm, *B*: 50 μm, *inset* in *B*: 25 μm.

ule cells is at equivalent to ≥0.5 mM EGTA, these data suggest that the inclusion of 0.5 mM EGTA does not affect these properties (in granule cells at least) under our experimental conditions. Furthermore, the physiological properties recorded remained generally stable over time, suggesting that any artifacts introduced by the pipette solution must occur immediately or be subtle; nevertheless, we cannot rule out the problem entirely. Finally, it should be noted that the properties examined here were measured in an attempt to identify electrophysiological signatures of the different types of hilar neurons in slices. In vivo, some of these properties are likely to differ, and the actual firing patterns of these neurons will depend on the nature of their synaptic and neuromodulatory inputs in the behaving animal.

Despite these shortcomings, the present study provides useful data concerning the physiological and morphological characteristics of distinct neuronal types in the hilar region of the rat fascia dentata. Moreover, at present the contribution of the various hilar cell types to hippocampal function in learning and memory is unknown. One way toward a better understanding of the role of the different cell types in the hilar region is by carefully monitoring both physiological and morphological characteristics of individual neurons (Buckmaster and Schwartzkroin 1995a,b; Halasy and Somogyi 1993; Han et al. 1993; Mott et al. 1997; Sik et al 1997).

Classification of cell types

In addition to the granule cells and basket cells, three major cell types are described: the mossy cell and the spiny and aspiny interneurons. Granule cells and mossy cells are likely to be excitatory, using glutamate as a neurotransmitter,

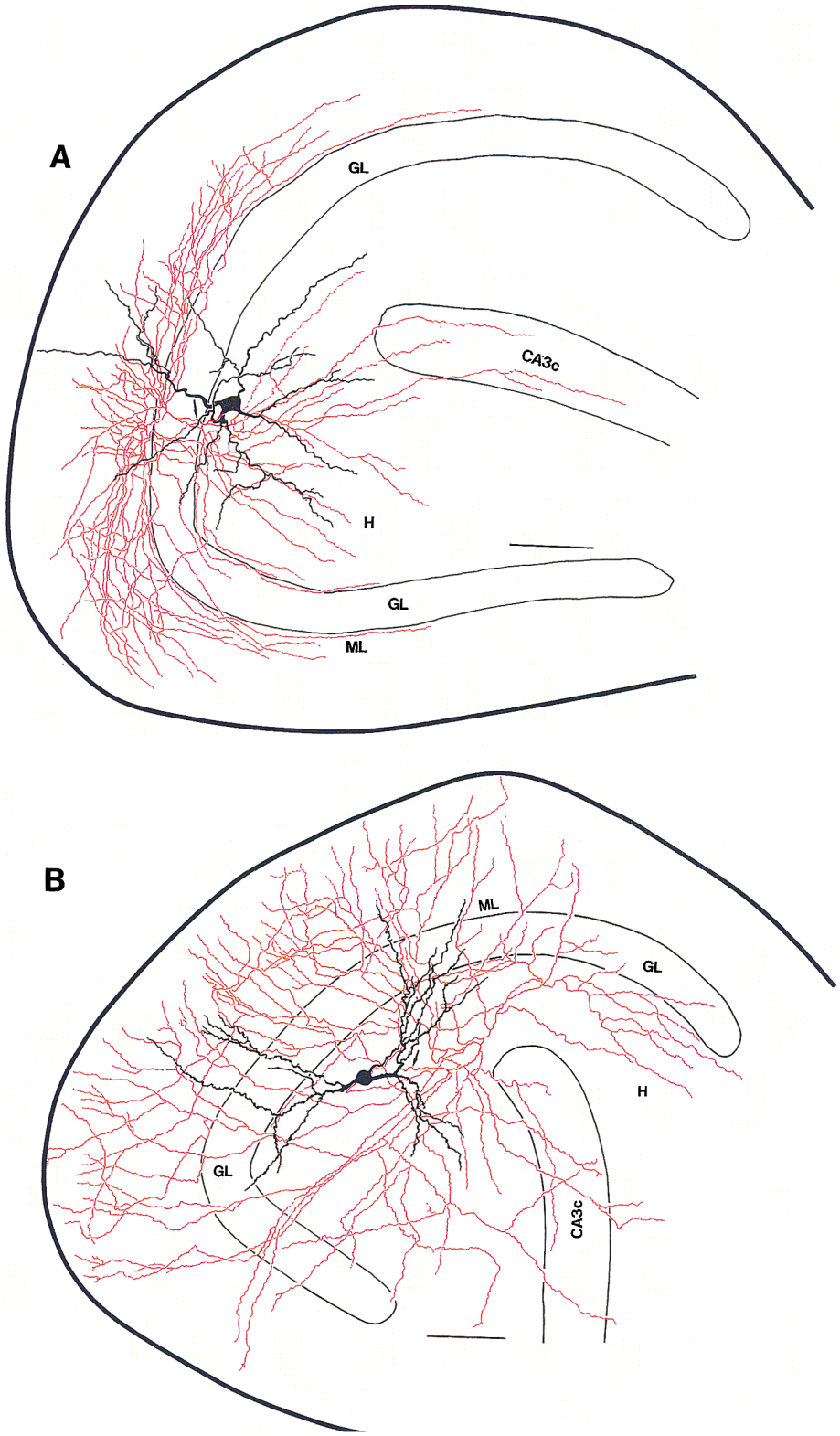

FIG. 8. Camera lucida reconstructions of 2 multipolar aspiny hilar interneurons. Arrows, origin of the axons; thick black lines indicate the pial surface. Note that the axonal projection (red) terminates mainly within the inner molecular layer closer to the granule cell layer (cell in *A*) and the outer molecular layer (cell in *B*). Both cells have a prominent axonal domain in the hilus and in CA3c. H, hilar region; GL, granule cell layer; ML, molecular layer. Scale bar: 100 μm.

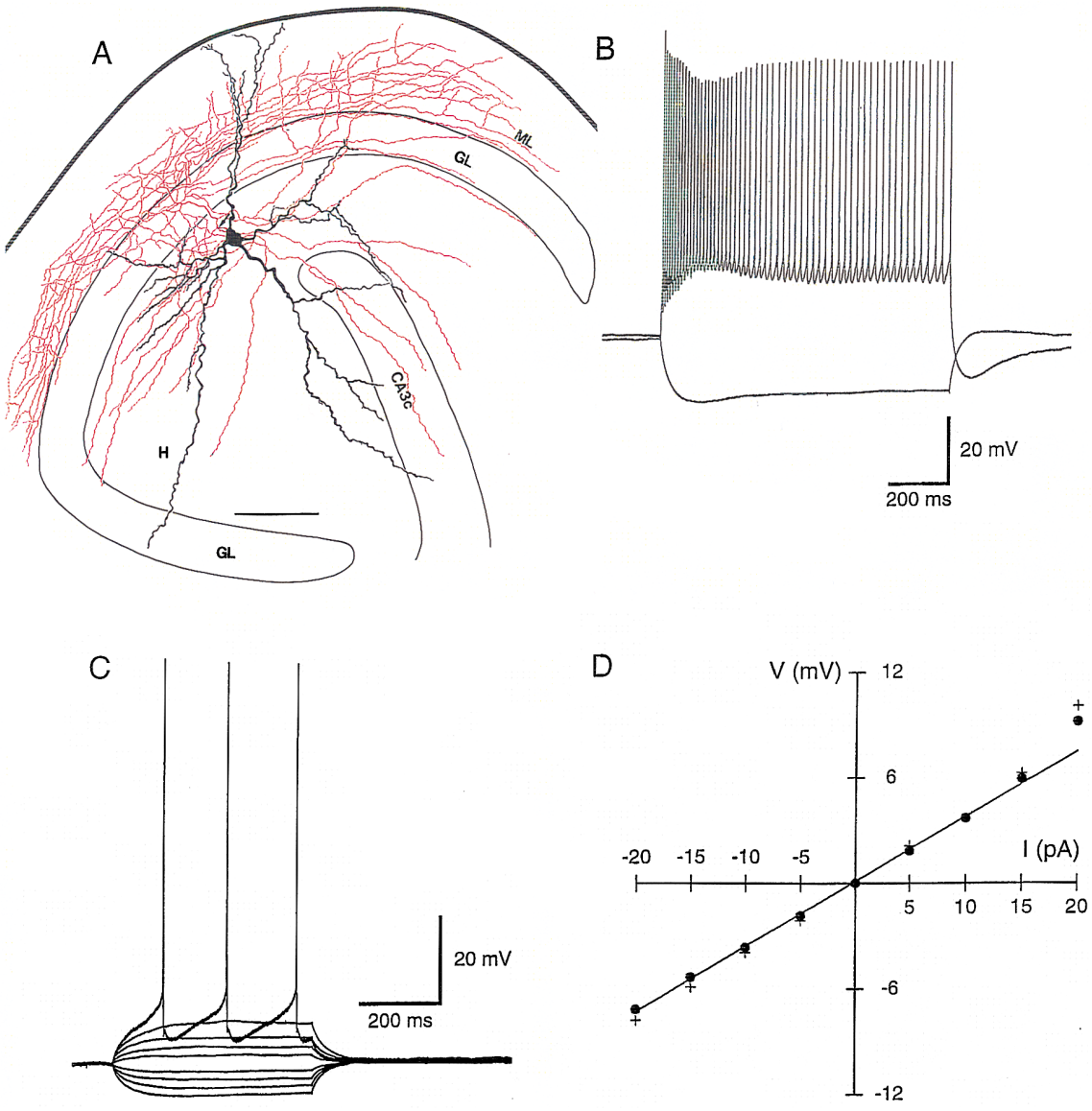

FIG. 9. Paired morphology and physiology of an aspiny hilar interneuron. *A*: morphology of the biocytin-filled neuron Axonal projection of the neuron (red) is confined mainly to the inner molecular layer. →, origin of the axon from the cell body; thick black line indicates the pial surface. H, hilar region; GL, granule cell layer; ML, molecular layer. Scale bar: 100 μm. *B*: responses to 1-s current injections of +200 and −50 pA. Maximum firing (58 Hz) was observed with the +200-pA current injection. Sag ratio = 0.84 (−50 pA response). *C*: voltage responses to current injections of −20 to +25 pA in 5-pA increments. All responses, except the action potentials, are averages of 4–5 trials. τ_o = 40 ms; action potential half-width = 0.55 ms. *D*: voltage-current relationship for the data shown in *C*. ●, steady state voltages; +, peak responses, most of which overlap; ——, linear regression through the steady state points between −20 and +15 pA. R_N = 369 MΩ; V_{rest} = −59 mV.

whereas basket cells and hilar interneurons are thought to be GABAergic inhibitory interneurons (e.g., Halasy and Somogyi 1993; Ribak et al. 1978; Sloviter and Nilaver 1987; Soriano and Frotscher 1993, 1994). Aspiny hilar interneurons can be subdivided further into those with a predominant projection to the inner molecular layer or the outer molecular layer. Other authors have adopted similar classification schemes for hilar neurons (Buckmaster and Schwartzkroin 1995a,b; Frotscher et al. 1994; Han et al. 1993; Mott et al. 1997; Seay-Lowe and Claiborne 1992; Sik et al. 1997; Soriano and Frotscher 1993). There is evidence that the various hilar neurons projecting to subzones of the molecular layer give rise to commissural fibers terminating in the same zones of the contralateral fascia dentata (Deller et al. 1995; see also Sik et al. 1997).

The aspiny hilar interneurons projecting to the inner molecular layer correspond to the HICAP cells (hilar interneurons with dense axonal plexus in the commissural/associational pathway terminal field) described by Han et al. (1993); at least some of these neurons could contain cholecystokinin (Fredens et al. 1987; Kosaka et al. 1985; Léránth and Frotscher 1986; Sloviter and Nilaver 1987; Somogyi et al. 1984; Stengaard-Pedersen et al. 1983). The aspiny hilar interneurons projecting to the outer molecular layer may

correspond to the HIPP cells (hilar interneurons with axons ramifying in the perforant path terminal field) described by Han et al. (1993), which are likely to contain neuropeptide Y (Deller and Léránth 1990) and/or somatostatin (Bakst et al. 1986; Léránth et al. 1990). However, as the axonal collaterals of these neurons traverse the entire molecular layer, they also may correspond to the cell with collaterals throughout the molecular layer described in Golgi preparations (Soriano and Frotscher 1993). Spiny hilar interneurons, like those stained in vivo by Buckmaster and Schwartzkroin (1995a,b), also may contain somatostatin (Bakst et al. 1986). We regard it as an important observation that all of the interneurons, except the basket cell, had additional axonal domains in the hilus and in CA3. These additional termination fields indicate that these neurons do not only act in a feedback manner on granule cell and basket cell dendrites but also have feedforward connections to other hilar and CA3 neurons. Moreover, in the absence of a detailed electron microscopic analysis, it cannot be excluded that the axons of spiny and aspiny neurons projecting to the OML give rise to numerous en passant synapses in the IML, which they traverse. The present classification of dentate hilar neurons is far from complete. In a Golgi study, Amaral (1978) described 21 neuronal cell types mainly on the basis of their dendritic configuration. Also, an important cell type, the dentate chandelier cell, was not encountered in our study. It recently has been described morphologically and physiologically in some detail (Buhl et al. 1994b; Soriano and Frotscher 1989; Soriano et al. 1990).

Physiological distinctions between cell types

The values of R_N and τ_o determined in our study are somewhat higher than determined with microelectrodes (Buckmaster and Schwartzkroin 1995a,b; Buckmaster et al. 1993a,b; Scharfman 1992; Scharfman and Schwartzkroin 1988) probably due to a leak conductance caused by microelectrode impalement (Spruston and Johnston 1992; Staley et al. 1992). A previous patch-clamp study of hilar neurons found similar R_N values to ours (Livsey and Vicini 1992). R_N and τ_o values may be effectively lower in vivo, however, because of the higher degree of spontaneous synaptic activity than in the slice (Buckmaster and Schwartzkroin 1995a,b).

In agreement with others, each of the types of neurons in our classification had distinct electrophysiological properties (Buckmaster and Schwartzkroin 1995a,b; Livsey and Vicini 1992; Mott et al. 1997; Scharfman 1992). The basket cells were easily distinguishable from other hilar neurons on the basis of their low R_N and τ_o, lack of sag in hyperpolarizing responses, and rapid maximum firing rate. Granule cells also could be distinguished reliably because they were the only other cell type to lack sag but had much higher R_N and τ_o and much lower maximum firing rates than basket cells. Because basket cells and granule cells can be distinguished readily from all other hilar cell types studied and from one another, we then only need consider further distinctions between mossy cells, spiny, and IML and OML aspiny interneurons.

The physiological properties of IML and OML aspiny neurons appeared generally similar, though our sample size for the OML aspiny neurons was too small to permit a statistical comparison. Hence, the statistical comparisons below compare other cell types to IML, but not OML, aspiny interneurons. Nevertheless, the similarity of these cells suggests that none of the properties measured would provide an accurate physiological signature of the axonal projection of aspiny hilar interneurons.

Spiny interneurons generally can be distinguished by their high R_N (higher than mossy cells) and small, slow AHP (smaller than aspiny interneurons). Despite these statistical differences, however, occasional errors in their identification could be made using these criteria because of some overlap in the ranges of these parameters with mossy cells and aspiny interneurons.

Mossy cells had a lower R_N than hilar interneurons, on average, but this difference was only statistically significant for mossy cells versus IML aspiny interneurons and not for mossy cells versus spiny interneurons. Furthermore, some overlap in the range was observed between R_N for mossy cells and each type of interneuron. The fast AHP was smaller in mossy cells than in spiny or aspiny interneurons (see also Livsey and Vicini 1992; Scharfman 1992), but again, there was considerable overlap in the ranges. The most reliable property for distinguishing mossy cells from aspiny hilar interneurons was the slow AHP after a train of action potentials, which was significantly larger for IML aspiny interneurons. Two aspiny interneurons, however, one IML and one OML, had slow AHPs as small as those of mossy cells; so even this property is not a perfect means of distinguishing mossy cells from aspiny hilar interneurons.

Using these guidelines, comparison of the measured physiological properties with the values given in Table 1 would allow successful physiological identification of cell type with a reasonably high probability. From our data set, the approximate expected failure rate for identification of the different hilar cell types would be: granule cells 0, basket cells 0, mossy cells 0.11, spiny interneurons 0, aspiny IML and OML interneurons 0.29.

Flow of information through the fascia dentata and hilus

As information arrives at the fascia dentata, it is segregated into inputs arriving via the associational/commissural afferents, medial perforant path, and lateral perforant path, which correspond to the inner, middle, and outer thirds of the molecular layer (e.g., Blackstad 1956; Steward 1976). It is likely that these inputs convey different information to the granule cells, which may integrate these synaptic inputs in different ways (for simplification, other inputs to the granule cells, i.e., subcortical afferents, are neglected here). In this context, it is interesting that hilar interneurons project back to the molecular layer in a laminated fashion. As these neurons are presumably inhibitory, neurons projecting specifically to the outer molecular layer would be in a position to selectively shut down inputs from lateral perforant path, whereas those projecting specifically to the inner molecular layer would be in a position to shut down inputs from the contralateral hippocampus. Medial perforant path inputs could be inhibited by either type, depending on the exact location of inhibitory afferents in the middle molecular layer. As action potential initiation occurs near the soma of granule cells (Jefferys 1978), however, inhibitory interneurons pro-

jecting to the inner molecular layer could reduce the efficacy of excitatory inputs in all parts of the molecular layer via shunting inhibition. Interneurons formed basket-like arrays of boutons on granule cell somata in addition to their laminar projections to the molecular layer, however, so if the laminar specificity of the projections to the molecular layer is of functional significance, one also might expect the somatic contacts to be somehow functionally distinct from the dendritic inputs arising from the same axons.

Another powerful source of inhibition of granule cells comes from basket cells. Because of the somatic location of synapses from basket cells and their ability to fire at very high rates, it is likely that basket cell activation completely blocks action potential firing in granule cells under some conditions. Furthermore, because of the extensive collateralization of basket cell axons in the granule cell layer, activation of a single basket cell would appear to be able to inhibit a large population of granule cells (Buhl et al. 1994a, 1995). Such widespread inhibition of granule cells may be a general feature of inhibitory interneurons in the dentate gyrus. The axon collaterals of spiny and aspiny interneurons projecting to the molecular layer were also widespread, and in vivo, these neurons have been shown to have longitudinal projections extending $\leq$50% of the length of the septotemporal axis of the hippocampal formation and even have some axon collaterals that extend into CA1 (Buckmaster and Schwartzkroin 1995a,b). The GABAergic dentate chandelier cell (Buhl et al. 1994b; Soriano and Frotscher 1989; Soriano et al. 1990) also contributes to the laminated inhibitory input of the granule cells by selectively contacting the axon initial segments of the granule cells.

Of particular interest will be to learn under what conditions basket cells are activated in vivo. As they also receive input from the perforant path (Zipp et al. 1989), one possibility is that they are activated by the same inputs that activate granule cells and that they then feedback and inhibit granule cell firing with a delay, thus effectively imposing a refractory period on granule cell firing. Arguing against this idea, however, is the fact that the lower R_N and τ_o of basket cells might make them less likely to integrate inputs over tens of milliseconds, as granule cells might, but would likely require synchronous synaptic inputs to bring them to firing threshold. Hence granule cell firing might be inhibited by basket cell activation only when basket cells are activated by many synchronous inputs. The ability of basket cells to fire rapidly and the low R_N and τ_o of basket cells, as well as the rapid kinetics of α-amino-3-hydroxy-5-methyl-4-isoxazolepropionic acid receptor channels in these neurons (Koh et al. 1995), imply that basket cells could reliably follow such synchronous inputs with action potential firing, even at very high frequencies, and possibly therefore provide a tonic form of granule cell inhibition (see Geiger et al. 1997).

Mossy cells receive their primary inputs directly from the granule cells via mossy fiber collaterals. Another source of inputs could come from any of the hilar neurons, which all have collaterals in the hilus. Mossy cells, which are believed to be excitatory (Scharfman 1995; Soriano and Frotscher 1994), constitute one of the output neurons of the hilus, as their axons project to the contralateral hippocampus (Frotscher et al. 1991; Ribak et al. 1985). As shown in the present study, mossy cells have extensive axon collaterals within the hilus, suggesting that their role as local circuit neurons is probably as important as their function as output neurons. These local circuits could constitute an excitatory feedback network onto granule cells, pyramidal cells, basket cells, or hilar interneurons. Buckmaster and Schwartzkroin (1994) propose that just such a positive feedback loop may form an associational circuit that is important for memory formation. Experimental evidence for a positive feedback circuit from mossy cells to granule cells comes from voltage-sensitive dye and microelectrode recordings, suggesting that mossy cells can mediate feedback excitation of granule cells (Jackson and Scharfman 1996; Scharfman 1995). However, they also may play an important role in polysynaptic feedback inhibition of granule cells as mossy cells were found to innervate interneurons (Scharfman 1995)—probably including both basket cells and spiny and aspiny interneurons. This connection could play a role in the hyperexcitability of granule cells during epilepsy because mossy cells are particularly sensitive to ischemia, and their death could lead to a reduction in inhibition of granule cells (loss of excitatory drive to inhibitory interneurons, cf. Sloviter 1987, 1991).

Both spiny and aspiny interneurons have extensive axon collaterals within the hilus. It seems likely that at least some of the inhibitory input of mossy cells could come from hilar interneurons (Buckmaster and Schwartzkroin 1994; Soltesz and Mody 1994). The unresolved targets and inputs of hilar interneurons are likely to be addressed in the future with recordings and reconstructions of pairs of neurons in slices (see Buhl et al. 1994a, 1995; Geiger et al. 1997; Miles et al. 1996; Scharfman 1994, 1995; Scharfman et al. 1990).

The authors are grateful to B. Joch, S. Nestel, and M. Winter for technical assistance and to T. Mickus for providing some granule cell data.

This work was supported by the von Helmholtz-Programm of the Bundesministerium für Bildung und Forschung (J. Lübke), the Alexander von Humboldt Foundation (N. Spruston), and the Deutsche Forschungsgemeinschaft Grant Fr 620/1-6 and Leibniz Programm (M. Frotscher).

Address for reprint requests: M. Frotscher, Anatomisches Institut der Universität Freiburg, PO Box 111, D-79001 Freiburg, Germany.

Received 15 July 1997; accepted in final form 27 October 1997.

REFERENCES

AMARAL, D. G. A Golgi study of cell types in the hilar region of the hippocampus in the rat. *J. Comp. Neurol*. 182: 851–914, 1978.

AMARAL, D. G. AND WITTER, M.P. The three-dimensional organization of the hippocampal formation. A review of anatomical data. *Neuroscience* 31: 571–591, 1989.

AMARAL, D. G. AND WITTER, M. P. The hippocampal formation. In: *The Rat Nervous System*, edited by G. Paxinos (2nd ed.). San Diego: Academic Press, 1995, p. 443–493.

BAKST, I., AVENDANO, C., MORRISON, J. H., AND AMARAL, D. G. An experimental analysis of the origins of somatostatin-like immunoreactivity in the dentate gyrus of the rat. *J. Neurosci.* 6: 1452–1462, 1986.

BENVENISTE, H. AND DIEMER, N. H. Early postischemic ^{45}Ca accumulation in rat dentate hilus. *J. Cereb. Blood Flow Metab.* 8: 713–719, 1988.

BLACKSTAD, T. W. Commissural connections of the hippocampal region in the rat, with special reference to their mode of termination. *J. Comp. Neurol.* 105: 417–537, 1956.

BUCKMASTER, P. S., KUNKEL, D. D., ROBBINS, R. J., AND SCHWARTZKROIN, P. A. Somatostatin-immunoreactivity in the hippocampus of the mouse, rat, guinea pig, and rabbit. *Hippocampus* 4: 167–180, 1994.

BUCKMASTER, P. S. AND SCHWARTZKROIN, P. A. Hippocampal mossy cell function: a speculative view. *Hippocampus* 4: 393–402, 1994.

BUCKMASTER, P. S. AND SCHWARTZKROIN, P. A. Interneurons and inhibition in the dentate gyrus of the rat in vivo. *J. Neurosci.* 15: 774–789, 1995a.

BUCKMASTER, P. S. AND SCHWARTZKROIN, P. A. Physiological and morphological heterogeneity of dentate gyrus-hilus interneurons in the gerbil hippocampus. *Eur. J. Neurosci.* 7: 1393–1402, 1995b.

BUCKMASTER, P. S., STROWBRIGDE, B. W., KUNKEL, D. D., SCHMIEGE, D. L., AND SCHWARTZKROIN, P. A. Mossy cell axonal projection to the dentate gyrus molecular layer in the rat hippocampal slice. *Hippocampus* 2: 349–362, 1993a.

BUCKMASTER, P. S., STROWBRIDGE, B. W., AND SCHWARTZKROIN, P. A. A comparison of rat hippocampal mossy cells and CA3c pyramidal cells. *J. Neurophysiol.* 70: 1281–1299, 1993b.

BUCKMASTER, P. S., WENZEL, H. J., KUNKEL, D. D., AND SCHWARTZKROIN, P. A. Axon abors and synaptic connections of hippocampal mossy cells in the rat in vivo. *J. Comp. Neurol.* 366: 270–292, 1996.

BUHL, E. H., COBB, S. R., HALASY, K., AND SOMOGYI, P. Properties of unitary IPSPs evoked by anatomically identified basket cells in the rat hippocampus. *Eur. J. Neurosci.* 7: 1989–2004, 1995.

BUHL, E.H., HALASY, K., AND SOMOGYI, P. Diverse sources of hippocampal unitary inhibitory postsynaptic potentials and the number of release sites. *Nature* 368: 823–828, 1994a.

BUHL, E. H., HAN, Z.-S., LÖRINCZI, Z., STEZHKA, V. V., KARNUP, S. V., AND SOMOGYI, P. Physiological properties of anatomically identified axo-axonic cells in the rat hippocampus. *J. Neurophysiol*. 71: 1289–1307, 1994b.

CAVAZOS, J. E. AND SUTULA, T. P. Progressive neuronal loss induced by kindling: a possible mechanism for mossy fiber synaptic reorganization and hippocampal sclerosis. *Brain Res.* 527: 1–6, 1990.

CLAIBORNE, B. J., AMARAL, D. G., AND COWAN, W. M. A light and electron microscopic analysis of the mossy fibers of the rat dentate gyrus. *J. Comp. Neurol.* 246: 435–458, 1986.

CLAIBORNE, B. J., AMARAL, D. G., AND COWAN, W. M. Quantitative, three-dimensional analysis of granule cell dendrites in the rat dentate gyrus. *J. Comp. Neurol.* 302: 206–219, 1990.

CRAIN, B. J., WESTERKAM, W. D., HARRISON, A. H., AND NADLER, J. V. Selective neuronal death after transient forebrain ischemia in the Mongolian gerbil: a silver impregnation study. *Neuroscience* 27: 387–402, 1988.

DE LANEROLLE, N. C., KIM, J. H., ROBBINS, R. J., AND SPENCER, D. D. Hippocampal interneuron loss and plasticity in human temporal lobe epilepsy. *Brain Res.* 495: 387–395, 1989.

DELLER, T. AND LÉRÁNTH, C. Synaptic connections of neuropeptide Y (NPY) immunoreactive neurons in the hilar area of the rat hippocampus. *J. Comp. Neurol.* 300: 433–447, 1990.

DELLER, T., NITSCH, R., AND FROTSCHER, M. *Phaseolus vulgaris*-leucoagglutinin (PHAL) tracing of commissural fibers to the rat fascia dentata: evidence for a previously unknown commissural projection to the outer molecular layer. *J. Comp. Neurol.* 352: 55–68, 1995.

FREDENS, K., STENGAARD-PEDERSEN, K., AND WALLACE, M. M. Localization of cholecystokinin in the dentate commissural-associational system of the mouse and rat. *Brain Res.* 401: 68–75, 1987.

FREUND, T. F. AND BUZSÁKI, G. Interneurons of the hippocampus. *Hippocampus* 6: 347–470, 1996.

FRICKE, R. A. AND PRINCE, D. A. Electrophysiology of dentate gyrus granule cells. *J. Neurophysiol.* 51: 195–209, 1984.

FROTSCHER, M., SCHLANDER, M., AND LÉRÁNTH, C. Cholinergic neurons in the hippocampus: a combined light and electron microscopic immunocytochemical study in the rat. *Cell Tissue Res.* 246: 293–301, 1986.

FROTSCHER, M., SERESS, L., SCHWERDTFEGER, W. K., AND BUHL, E. H. The mossy cells of the fascia dentata: a comparative study of their fine structure and synaptic connections in rodents and primates. *J. Comp. Neurol.* 312: 145–163, 1991.

FROTSCHER, M., SORIANO, E., AND MISGELD, U. Divergence of hippocampal mossy fibers. *Synapse* 16: 148–160, 1994.

GEIGER, J.R.P., LÜBKE, J., ROTH, A., FROTSCHER, M., AND JONAS, P. Submillisecond AMPA receptor-mediated signaling at a principal neuron-interneuron synapse. *Neuron* 18: 1009–1023, 1997.

HALASY, K. AND SOMOGYI, P. Subdivisions in the multiple GABAergic innervation of granule cells in the dentate gyrus of the rat hippocampus. *Eur. J. Neurosci.* 5: 411–429, 1993.

HAN, Z.-S., BUHL, E. H., LÖRINCZI, Z., AND P. SOMOGYI, P. A high degree of spatial selectivity in the axonal and dendritic domains of physiologically identified local-circuit neurons in the dentate gyrus of the rat hippocampus. *Eur. J. Neurosci.* 5: 395–410, 1993.

HENDRY, S.H.C. AND JONES, D. J. Morphology of synapses formed by cholecystokinin-immunoreactive axon terminals in regio superior of rat hippocampus. *Neuroscience* 16: 57–68, 1985.

HSU, I., AND BUZSÁKI, G. Vulnerability of mossy fiber targets in the rat hippocampus to forebrain ischemia. *J. Neurosci.* 13: 3964–3979, 1993.

JACKSON, M. B. AND SCHARFMAN, H.E. Positive feedback from hilar mossy cells to granule cells in the dentate gyrus revealed by voltage-sensitive dye and microelectrode recording. *J. Neurophysiol.* 76: 601–616, 1996.

JEFFERYS, J.G.R. Initiation and spread of action potentials in granule cells maintained in vitro in slices of guinea-pig hippocampus. *J. Physiol. (Lond.)* 289: 375–388, 1978.

JONAS, P., MAJOR, G., AND SAKMANN, B. Quantal components of unitary EPSCs at the mossy fibre synapse on CA3 pyramidal cells of the rat hippocampus. *J. Physiol. (Lond.)* 472: 615–663, 1993.

KOH, D.-S., GEIGER, J.R.P., JONAS, P., AND SAKMANN, B. Ca^{2+}-permeable AMPA and NMDA receptor channels in basket cells of the rat hippocampal dentate gyrus. *J. Physiol. (Lond.)* 485: 383–402, 1995.

KOSAKA, T., KOSAKA, K., TATEISHI, K., HAMAOKA, Y., YANAIHARA, N., WU, J.-Y., AND HAMA, K. GABAergic neurons containing CCK-8-like and/or VIP-immunoreactivities in the rat hippocampus and dentate gyrus. *J. Comp. Neurol.* 239: 420–430, 1985.

LÉRÁNTH, C. AND FROTSCHER, M. Synaptic connections of cholecystokinin-immunoreactive neurons and terminals in the rat fascia dentata: a combined light and electron microscopic study. *J. Comp. Neurol.* 254: 51–64, 1986.

LÉRÁNTH, C., FROTSCHER, M., AND RAKIC, P. CCK-immunoreactive terminals form different types of synapses in the rat and monkey hippocampus. *Histochemistry* 88: 343–352, 1988.

LÉRÁNTH, C., FROTSCHER, M., TOMBÖL, T., AND PALKOVITS, P. Ultrastructure and synaptic connections of vasoactive intestinal polypeptide-like immunoreactive neurons and axon terminals in the rat hippocampus. *Neuroscience* 12: 531–542, 1984.

LÉRÁNTH, C., MALCOLM, A. J., AND FROTSCHER, M. Afferent and efferent synaptic connections of somatostatin-immunoreactive neurons in the rat fascia dentata. *J. Comp. Neurol.* 295: 111–122, 1990.

LI, X.-G., SOMOGYI, P., YLINEN, A., AND BUSZÁKI, G. The hippocampal CA3 network: an in vivo intracellular labeling study. *J. Comp. Neurol.* 339: 181–208, 1994.

LINDSAY, R. D. AND SCHEIBEL, A. B. Quantitative analysis of the dendritic branching pattern of granule cells from adult rat dentate gyrus. *Exp. Neurol.* 73: 286–297, 1981.

LIVSEY, C. T. AND VICINI, S. Slower spontaneous excitatory postsynaptic currents in spiny versus aspiny hilar neurons. *Neuron* 8: 745–755, 1992.

LORENTE DE NÓ, R. Studies on the structure of the cerebral cortex. II. Continuation of the study of the ammonic system. *J. Psychol. Neurol. Leipzig* 46: 113–177, 1934.

LÜBBERS, K. AND FROTSCHER, M. Fine structure and synaptic connections of identified neurons in the rat fascia dentata. *Anat. Embryol.* 177: 1–14, 1987.

LÜBKE, J., MARKRAM, H., FROTSCHER, M., AND SAKMANN, B. Frequency and dendritic distribution of autapses established by layer 5 pyramidal neurons in the developing rat neocortex: comparison with synaptic innervation of adjacent neurons of the same class. *J. Neurosci.* 16: 3209–3218, 1996.

MADISON, D. V. AND NICOLL, R. A. Control of the repetitive discharge of rat CA1 pyramidal neurones *in vitro*. *J. Physiol. (Lond.)* 354: 319–331, 1984.

MILES, R., TÓTH, K., GULYÁS, A. I., HÁJOS, H., AND FREUND, T. F. Differences between somatic and dendritic inhibition in the hippocampus. *Neuron* 16: 815–823, 1996.

MOTT, D. D., TURNER, D. A., OKAZAKI, M. M., AND LEWIS, D. V. Interneurons of the dentate-hilus border of the dentate gyrus: morphological and electrophysiological heterogeneity. *J. Neurosci.* 17: 3990–4005, 1997.

RAMÓN Y CAJAL, S. *Histologie du Systéme Nerveux de l'Homme et des Vertebrés.* Paris, Maloine, 1911.

RIBAK, C. E. AND SERESS, L. Five types of basket cell in the hippocampal dentate gyrus: a combined Golgi and electron microscopic study. *J. Neurocytol.* 12: 577–597, 1983.

RIBAK, C. E. AND SERESS, L. A Golgi-electron microscopic study of the fusiform neurons in the hilar region of the dentate gyrus. *J. Comp. Neurol.* 271: 67–78, 1988.

RIBAK, C. E., SERESS, L., AND AMARAL, D. G. The development, ultrastructure and synaptic connections of the mossy cells of the dentate gyrus. *J. Neurocytol.* 14: 835–857, 1985.

RIBAK, C. E., VAUGHN, J. E., AND SAITO, K. Immunocytochemical localization of glutamic acid decarboxylase in neuronal somata following colchicine inhibition of axonal transport. *Brain Res.* 140: 315–332, 1978.

SCHARFMAN, H. E. Differentiation of rat dentate neurons by morphology and electrophysiology in hippocampal slices: granule cells, spiny hilar cells, and aspiny fast-spiking cells. In: *The Dentate Gyrus and its Role in Seizures*, edited by C. E. Ribak, C. M. Gall, and I. Mody. Amsterdam: Elsevier, 1992, p. 93–109.

SCHARFMAN, H. E. Synchronization of area CA3 hippocampal pyramidal cells and non-granule cells of the dentate gyrus in bicuculline-treated rat hippocampal slices. *Neuroscience* 59: 245–257, 1994.

SCHARFMAN, H. E. Electrophysiological evidence that dentate hilar mossy cells are excitatory and innervate both granule cells and interneurons. *J. Neurophysiol.* 74: 179–194, 1995.

SCHARFMAN, H. E., KUNKEL, D. D., AND SCHWARTZKROIN, P. A. Synaptic connections of dentate granule cells and hilar neurons: results of paired intracellular recordings and intracellular horseradish peroxidase injections. *Neuroscience* 37: 693–707, 1990.

SCHARFMAN, H. E. AND SCHWARTZKROIN, P. A. Electrophysiology of morphologically identified mossy cells of the dentate hilus recorded in guinea pig hippocampal slices. *J. Neurosci.* 8: 3812–3821, 1988.

SCHARFMAN, H. E. AND SCHWARTZKROIN, P. A. Responses of cells in the rat fascia dentata to prolonged stimulation of the perforant path: sensitivity of hilar cells and changes in granule cell excitability. *Neuroscience* 35: 491–504, 1990.

SEAY-LOWE, S. L. AND CLAIBORNE, B. J. Morphology of intracellularly labeled interneurons in the dentate gyrus of immature rat. *J. Comp. Neurol.* 324: 23–36, 1992.

SERESS, L. AND FROTSCHER, M. Basket cells in the monkey fascia dentata: a Golgi/electron microscopic study. *J. Neurocytol.* 20: 915–928, 1991.

SERESS, L. AND POKORNY, J. Structure of the granule cell layer of the rat dentate gyrus. A light microscopic and Golgi-study. *J. Anat.* 133: 181–195, 1981.

SIK, A., PENTTONEN, M., AND BUSZÁKI, G. Interneurons in the hippocampal dentate gyrus: an in vivo intracellular study. *Eur. J. Neurosci.* 9: 573–588, 1997.

SIK, A., TAMAMAKI, N., AND FREUND, T. F. Complete axonal arborization of a single CA3 pyramidal cell in the rat hippocampus, and its relationship with postsynaptic parvalbumin-containing interneurons. *Eur. J. Neurosci.* 5: 1719–1728, 1993.

SLOVITER, R. S. Decreased hippocampal inhibition and a selective loss of interneurons in experimental epilepsy. *Science* 235: 73–76, 1987.

SLOVITER, R. S. Permanently altered hippocampal structure, excitability, and inhibition after experimental status epilepticus in the rat: the ''dormant basket cell'' hypothesis and its possible relevance to temporal lobe epilepsy. *Hippocampus* 1: 41–66, 1991.

SLOVITER, R. S. AND NILAVER, G. Immunocytochemical localization of GABA-, cholecystokinin, vasoactive intestinal polypeptide-, and somatostatin-like immunoreactivity in the area dentata and hippocampus of the rat. *J. Comp. Neurol.* 256: 42–60, 1987.

SOLTESZ, I. AND MODY, I. Patch-clamp recordings reveal powerful GABAergic inhibition in dentate hilar neurons. *J. Neurosci.* 14: 2365–2376, 1994.

SORIANO, E. AND FROTSCHER, M. A GABAergic axo-axonic cell in the fascia dentata controls the main excitatory hippocampal pathway. *Brain Res.* 503: 170–174, 1989.

SORIANO, E. AND FROTSCHER, M. GABAergic innervation of the rat fascia dentata: a novel type of interneuron in the granule cell layer with extensive axonal arborization in the molecular layer. *J. Comp. Neurol.* 334: 385–396, 1993.

SORIANO, E. AND FROTSCHER, M. Mossy cells of the rat fascia dentata are glutamate-immunoreactive. *Hippocampus* 4: 65–69, 1994.

SORIANO, E., NITSCH, R., AND FROTSCHER, M. Axo-axonic chandelier cells in the rat fascia dentata: Golgi-electron microscopy and immunocytochemical studies. *J. Comp. Neurol.* 293: 1–25, 1990.

SOMOGYI, P., HODGSON, A. J., SMITH, A. D., NUNZI, M. G., GORIO, A., AND WU, J.-Y. Different populations of GABAergic neurons in the visual cortex and hippocampus of the cat contain somatostatin- or cholecystokinin-immunoreactive material. *J. Neurosci.* 4: 2590–2603, 1984.

SPIGELMAN, I., ZHANG, L., AND CARLEN, P. L. Patch-clamp study of postnatal development of CA1 neurons in the rat hippocampal slices: membrane excitability and K^+ currents. *J. Neurophysiol.* 68: 55–69, 1992.

SPRUSTON, N. AND JOHNSTON, D. Perforated patch-clamp analysis of the passive membrane properties of three classes of hippocampal neurons. *J. Neurophysiol.* 67: 508–529, 1992.

SPRUSTON, N., LÜBKE, J., AND FROTSCHER, M. Diversity of nonprincipal cell types in the stratum lucidum of hippocampus: an anatomical and physiological characterization. *J. Comp. Neurol.* 385: 427–440, 1997.

STALEY, K. J., OTIS, T. S., AND MODY, I. Membrane properties of dentate gyrus granule cells: comparison of sharp microelectrode and whole-cell recordings. *J. Neurophysiol.* 67: 1346–1358, 1992.

STENGAARD-PEDERSEN, K., FREDENS, K., AND LARSSON, L.-L. Comparative localization of enkephalin and cholecystokinin immunoreactivities and heavy metals in the hippocampus. *Brain Res.* 273: 81–96, 1983.

STEWARD, O. Topographic organization of the projections from the entorhinal area to the hippocampal formation in the rat. *J. Comp. Neurol.* 167: 285–314, 1976.

STORM, J. F. Action potential repolarization and a fast after-hyperpolarization in rat hippocampal pyramidal cells. *J. Physiol. (Lond.)* 385: 733–759, 1984.

STUART, G.J., DODT, H.-U., AND SAKMANN, B. Patch-clamp recordings from the soma and dendrites of neurons in brain slices using infrared video microscopy. *Pflügers Arch.* 423: 511–518, 1993.

ZIPP, F., NITSCH, R., SORIANO, E., AND FROTSCHER, M. Entorhinal fibers form synaptic contacts on parvalbumin-immunoreactive neurons in the rat fascia dentata. *Brain Res.* 495: 161–166, 1989.